Electronic Supplementary Information

Molecular or dissociative adsorption of water on the clean and oxygen pre-covered Ni(111) surface

Ling Zhu,[a,b,c] Chunli, Liu;[a,b,c] Xiaodong Wen[a,b] Yong-Wang Li,[a,b] Haijun Jiao[a,d]*

a) State Key Laboratory of Coal Conversion, Institute of Coal Chemistry, Chinese Academy of Sciences, Taiyuan, 030001, China; b) National Energy Center for Coal to Liquids, Synfuels China Co., Ltd, Huairou District, Beijing, 101400, China; c) University of Chinese Academy of Sciences, No. 19A Yuquan Road, Beijing, 100049, PR China; d) Leibniz-Institut für Katalyse e.V. an der Universität Rostock, Albert-Einstein Strasse 29a, 18059 Rostock, Germany. E-mail: haijun.jiao@catalysis.de

Adsorption energies and structural parameters of $(H_2O)_n$ adsorption (Table S1, Figure S1); dissociation energetics of H_2O and $(H_2O)_2$ on the clean surface (Tables S2-S3; Figures S2-S3) as well as on the oxygen pre-covered surface (Tables S4-S5; Figures S4-S6); stretching and bending frequencies of 4O, $(OH)_n$, $4O+4H_2O$ and $(H_2O)_n$ on Ni(111) (Table S6); potential energy surface of H_2O dissociative adsorption on 3O and 4O pre-covered surfaces (Figure S7); high coverage OH and O adsorption configurations and energies (Figures S8-S12; Figure S13).

Table S1. PBE-D3 computed adsorption energy (E_{ads}, eV), Ni-O ($d_{O\text{-}Ni,}$ Å) and H-bonding distances ($d_{H\text{-}bond,}$ Å) of $(H_2O)_n$ clusters on Ni(111) surface

	E_{ads}	$d_{Ni\text{-}O}$	$d_{H\text{-}bond}$
$(H_2O)_1$	−0.42	2.156	
$(H_2O)_2$	−1.11	2.061; 3.031	1.687
$(H_2O)_3$	−1.77	2.005; 3.028; 3.026	1.727; 1.727
$(H_2O)_4$	−2.50	2.101; 2.065; 2.910; 2.924	1.678; 1.668; 1.668
$(H_2O)_5$	−3.10	2.193; 1.990; 3.120; 2.957; 3.171	1.919; 1.681; 1,698; 1.859; 1.749
$(H_2O)_{6\text{-}t1}$	−3.88	2.149; 2.150; 2.151; 2.984; 2.972; 2.978	1.796; 1.567; 1.798; 1.567; 1.797; 1.567
$(H_2O)_{6\text{-}t2}$	−3.87	2.167; 2.094; 2.233; 3.240; 2.985; 3.018	1.698; 1.618; 1.831; 1.644; 1.675; 2.113
$(H_2O)_{7\text{-}t1}$	−4.57	2.221; 2.021; 2.115; 3.069; 3.045; 2.964; 3.162	1.819; 1.794; 1.692; 1.809; 1.634; 1.825; 1.842
$(H_2O)_{7\text{-}t2}$	−4.46	2.064; 2.136; 2.196; 2.956; 2.978; 2.980; 3.301	1.645; 1.740; 1.518; 1.787; 1.671; 1.841; 1.632
$(H_2O)_8$	−5.26	2.050; 2.215; 2.135; 2.983; 2.966; 2.998; 3.333; 3.717	1.602; 1.746; 1.657; 1.813; 1.778; 1.808; 1.860; 1.776

Figure S1. RPBE-D3 adsorption energy (eV) of $(H_2O)_n$ clusters on Ni(111) (Ni/blue; O/red; H/white; small O atoms for shorter Ni-O distance and large O atoms for longer Ni-O distance) (where RPBE-D3 single-point energy with the PBE optimized structure as well as PBE zero-point energy)

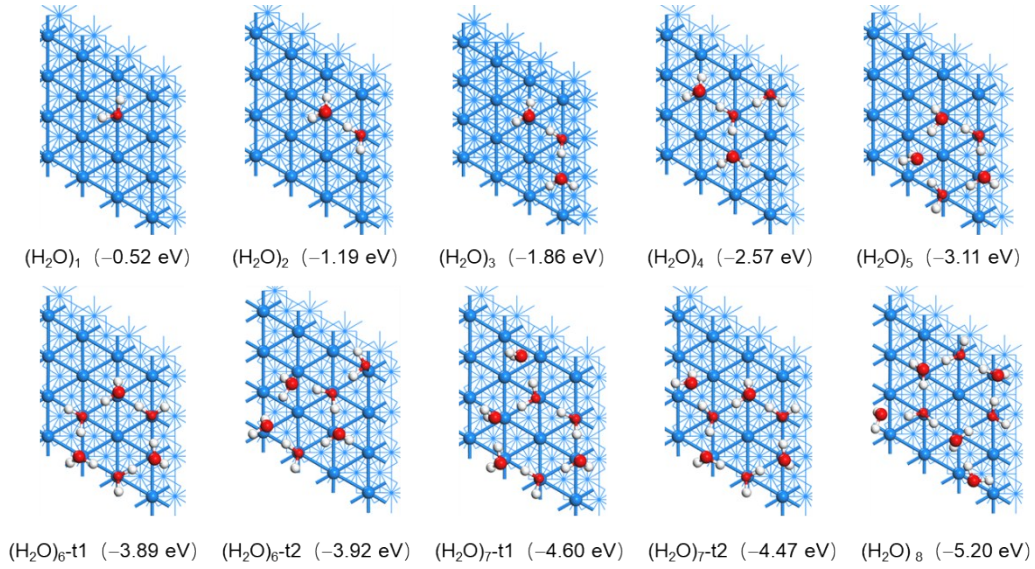

Figure S2. PBE-D3 optimized structures and the adsorption energy (eV) of $2H_2O$ dissociation for the stationary points on Ni(111) surface (Ni/blue; O/red; H/white; small O atoms for shorter Ni-O distance and large O atoms for longer Ni-O distance).

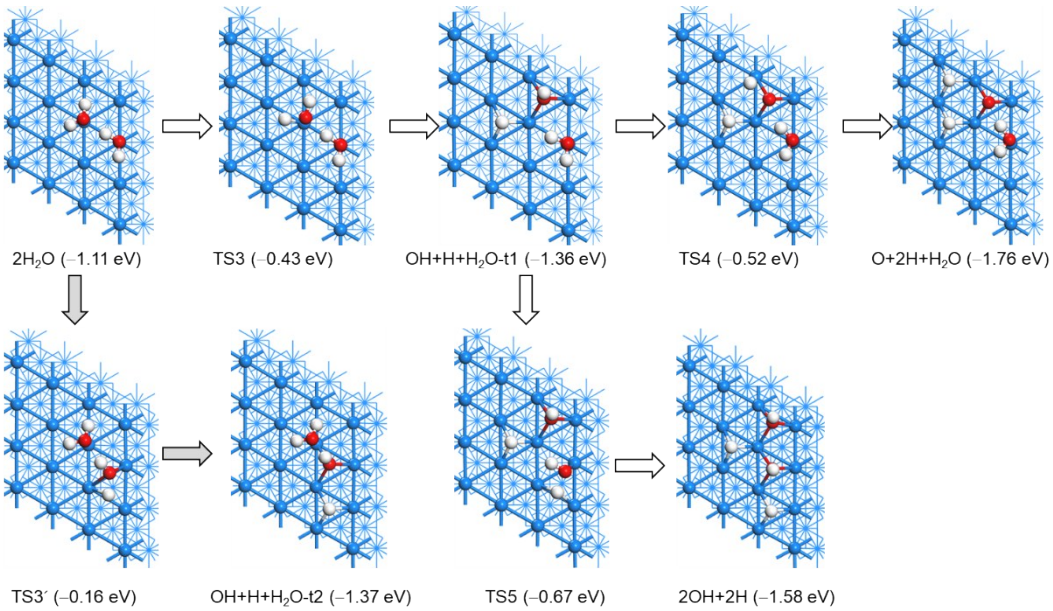

Table S2. Adsorption energy (E_{ads}, eV) and shortest distances (d, Å) of the IS and FS for H_2O direct dissociation and $2H_2O$ dissociation on Ni(111) surface using PBE-D3

	E_{ads}	d_{Ni-O}	d_{Ni-H}
		H_2O direct dissociation	
H_2O	−0.42	2.156	
OH+H	−0.98	1.943; 1.966; 2.001	1.655; 1.714; 1.749
O+2H	−1.16	1.821; 1.821; 1.888	1.663; 1.698; 1.729; 1.663; 1.699; 1.729
		$2H_2O$ dissociation	
H_2O+H_2O	−1.11	2.057; 3.021	
H_2O+OH+H	−1.36	1.964; 1.980; 2.056; 2.155	1.656; 1.713; 1.737
H_2O+O+2H	−1.76	1.834; 1.893; 1.900; 2.096	1.649; 1.705; 1.756; 1.646; 1.701; 1.757
2OH+2H	−1.58	1.933; 1.952; 2.107; 1.934; 1.973; 2.001	1.673; 1.678; 1.773; 1.635; 1.712; 1.769

Table S3. PBE-D3 computed dissociation barriers and energies (E_a and E_r, eV), bond distances (d_{Ni-X}, Å) and the breaking O-H bond distance (d_{O-H}, Å) in the transition state for H_2O direct dissociation and $2H_2O$ dissociation on Ni(111) surface

	E_a	E_r	d_{Ni-O}	d_{Ni-H}	d_{O-H}
			$H_2O \rightarrow TS1 \rightarrow OH + H$		
TS1	0.68	−0.56	1.931	1.736; 1.760	1.544
			$OH + H \rightarrow TS2 \rightarrow O + 2H$		
TS2	1.25	−0.18	1.885; 2.005; 2.079	1.666; 1.663; 1.682; 1.737	1.555
			$2H_2O \rightarrow TS3 \rightarrow H_2O + OH + H$		
TS3	0.68	−0.25	2.041; 2.072	1.665	1.475
			$H_2O + OH + H \rightarrow TS4 \rightarrow H_2O + O + 2H$		
TS4	0.84	−0.40	2.104; 1.901; 1.932; 1.952	1.528; 1.646; 1.703; 1.764	1.478
			$H_2O + OH + H \rightarrow TS5 \rightarrow 2OH + 2H$		
TS5	0.69	−0.22	1.960; 1.949; 1.952; 2.058	1.719; 1.734; 1.660; 1.714; 1.742	1.512

Table S4. PBE-D3 computed adsorption energies (E_{ads}, eV) and bond lengths (d_{Ni-X}, Å) of the IS and FS for H_2O dissociation on O pre-covered Ni(111)

	E_{ads}	d_{Ni-O}	d_{Ni-H}
		1O assisted H_2O dissociation	
O+H_2O	−0.80	1.864; 1.866; 1.877; 2.105	
2OH	−0.66	1.934; 1.965; 2.040; 1.934; 1.966; 2.043	
O+H+OH	−0.81	1.908; 1.981; 2.039; 1.804; 1.856; 1.891	1.633; 1.728; 1.729
2O+2H	−0.85	1.791; 1.852; 1.874; 1.789; 1.850; 1.876	1.641; 1.706; 1.725; 1.654; 1.695; 1.730
		2O assisted H_2O dissociation	
2O+H_2O	−0.96	1.824; 1.866; 1.913; 2.106	
O+2OH	−0.88	1.939; 1.941; 2.065; 1.939; 1.942; 2.068	
2O+H+OH	−0.94	1.816; 1.831; 1.868; 1.933; 1.940; 2.079	1.632; 1.723; 1.737
3O+2H	−0.88	1.796; 1.849; 1.853; 1.799; 1.831; 1.885	1.640; 1.702; 1.733; 1.638; 1.702; 1.722
		3O assisted H_2O dissociation	
3O+H_2O	−0.71	1.813; 1.871; 1.908; 2.105	
2O+2OH	−0.53	1.926; 1.940; 2.073; 1.938; 1.938; 2.105	
3O+H+OH	−0.35	1.822; 1.826; 1.860; 1.929; 1.933; 2.125	1.632; 1.634; 1.754
4O+2H	−0.23	1.801; 1.844; 1.851; 1.796; 1.826; 1.960	1.630; 1.644; 1.724; 1.636; 1.696; 1.729
		4O assisted H_2O dissociation	
4O+H_2O	−0.82	1.863; 1.864; 1.868; 2.101	
3O+2OH	−0.68	1.929; 1.962; 2.034; 1.936; 1.959; 2.037	
4O+H+OH	−0.59	1.917; 1.955; 2.048; 1.814; 1.852; 1.866	1.650; 1.657; 1.732
5O+2H	−0.38	1.792; 1.846; 1.866; 1.792; 1.848; 1.862	1.650; 1.662; 1.714; 1.649; 1.667; 1.670

Table S5. PBE-D3 computed energy barriers and reaction energies (E_a and E_r, eV), bond distances (d_{Ni-X}, Å) and the breaking O-H bond distances (d_{O-H}, Å) of the TS for H_2O dissociation on O pre-covered Ni(111) surface

	E_a	E_r	d_{Ni-O}	d_{Ni-H}	d_{O-H}
			$1O + H_2O \rightarrow TS6 \rightarrow 2OH$		
TS6	0.46	0.14	1.930; 1.987; 1.994; 1.895		1.558
			$2OH \rightarrow TS7 \rightarrow O + H + OH$		
TS7	0.99	−0.15	1.858; 1.920;1.949; 1.925; 1.961; 2.038	1.507	1.490
			$O + H + OH \rightarrow TS8 \rightarrow 2O + 2H$		
TS8	1.16	−0.04	1.796; 1.847; 1.888; 1.841; 1.975; 2.035	1.640; 1.672; 1.731; 1.536	1.486
			$2O + H_2O \rightarrow TS9 \rightarrow O + 2OH$		
TS9	0.37	0.08	1.885; 1.995; 2.087; 1.900		1.530
			$O + 2OH \rightarrow TS10 \rightarrow 2O + H + OH$		
TS10	0.99	−0.06	1.885; 1.911; 2.005; 1.935; 1.940; 2.056	1.707; 1.708	1.400
			$2O + H + OH \rightarrow TS11 \rightarrow 3 + 2H$		
TS11	1.19	0.06	1.873; 1.900; 1.938; 1.806,; 1.834; 1.859	1.631; 1.726; 1.750; 1.556	1.489
			$3O + H_2O \rightarrow TS12 \rightarrow 2O + 2OH$		
TS12	0.45	0.18	1.878; 2.017; 2.097; 1.886		1.698
			$2O + 2OH \rightarrow TS13 \rightarrow 3O + H + OH$		
TS13	0.93	0.18	1.880; 1.911; 1.986; 1.930; 1.933; 2.113	1.558	1.434
			$3O + H + OH \rightarrow TS14 \rightarrow 4O + 2H$		
TS14	1.29	0.12	1.810; 1.827; 1.857; 1.856; 1.894; 1.989	1.634; 1.646; 1.754; 1.708	1.449
			$4O + H_2O \rightarrow TS15 \rightarrow 3O + 2OH$		
TS15	0.46	0.14	1.923; 1.972; 1.995; 1.907		1.507
			$3O + 2OH \rightarrow TS16 \rightarrow 4O + H + OH$		
TS16	0.90	0.09	1.921; 1.952; 2.030; 1.841; 1.951; 1.964	1.584	1.452
			$4O + H + OH \rightarrow TS17 \rightarrow 5O + 2H$		
TS17	1.19	0.21	1.870; 1.890; 1.923; 1.796; 1.853; 1.859	1.654; 1.663; 1.715; 1.516	1.510

Table S6. Stretching and bending frequencies (cm^{-1}) of 4O (0.25 ML), $(OH)_n$ (n = 1-4, 8), $4O+4H_2O$ on Ni(111) and $(H_2O)_n$ (n = 1-6)

Stable adsorption configurations	O-H stretching	O-H bending	O-Ni stretching
$1H_2O$	3700; 3584	1556	
$2H_2O$	3620;3699; 3552-3005	1610; 1576	
$3H_2O$	3646; 3641; 3163; 3564; 3549; 3125	1626; 1576; 1570	
$4H_2O$	3686; 3567; 3546; 3486; 3456; 3097; 2968; 2928	1625; 1580; 1562; 1559	
$5H_2O$	3704; 3672; 3514; 3506; 3445; 3432; 3141; 3054; 3010; 2986	1644; 1596; 1586; 1573; 1511	
$6H_2O$	3654; 3650; 3649; 3388 3380; 3363; 3315; 3314 3311; 2613; 2595; 2557	1635; 1622; 1620; 1586; 1583; 1574	
0.25 ML O (4O)			497;489; 487; 480
$4O + 4H_2O$ (top site)	3552; 3549; 3546; 3544 3445; 3443; 3442; 3440	1551; 1545; 1544; 1534	474; 464; 459; 446
1OH	3718		392
2OH	3709; 3705		395; 388
3OH	3706; 3700; 3699		398; 396; 390
4OH (0.25 ML)	3710; 3701; 3698; 3696		398; 393; 390; 381
8OH (0.50 ML)	3624; 3584; 3532; 3472; 3488; 3434; 3430; 3423		431; 411; 407; 393; 389; 391; 381; 365

Figure S3. Optimized structures and the adsorption energy (eV) H_2O dissociation for the stationary points on the O pre-covered Ni(111) surface (Ni/blue; O/red; H/white)

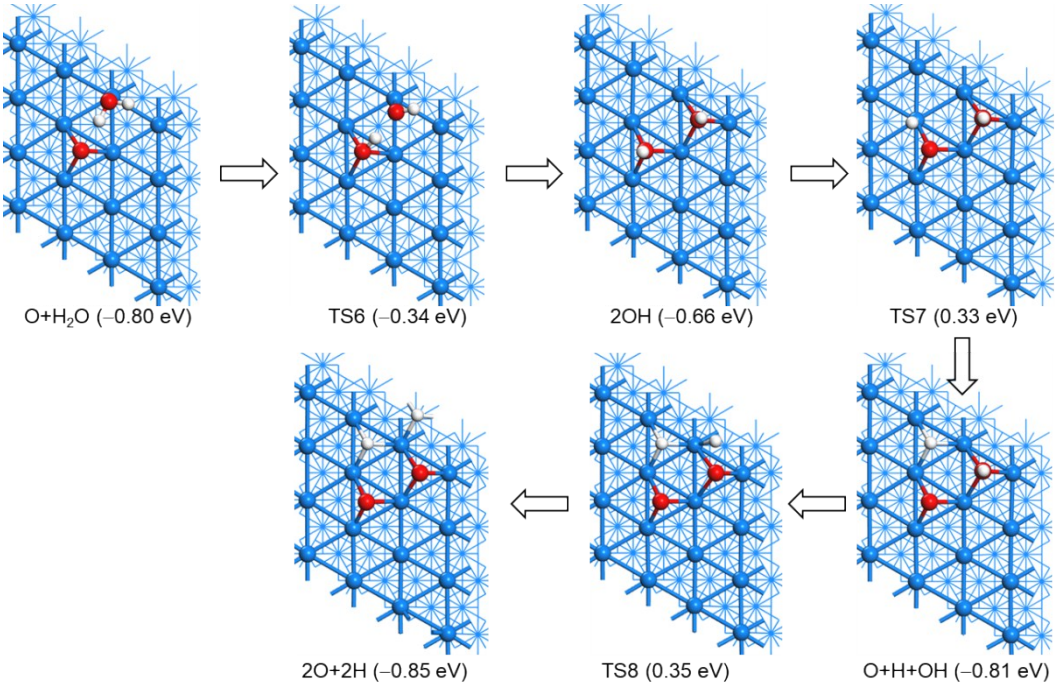

Figure S4. Optimized structures and the adsorption energy (eV) H_2O dissociation for the stationary points on the 2O pre-covered Ni(111) surface (Ni/blue; O/red; H/white).

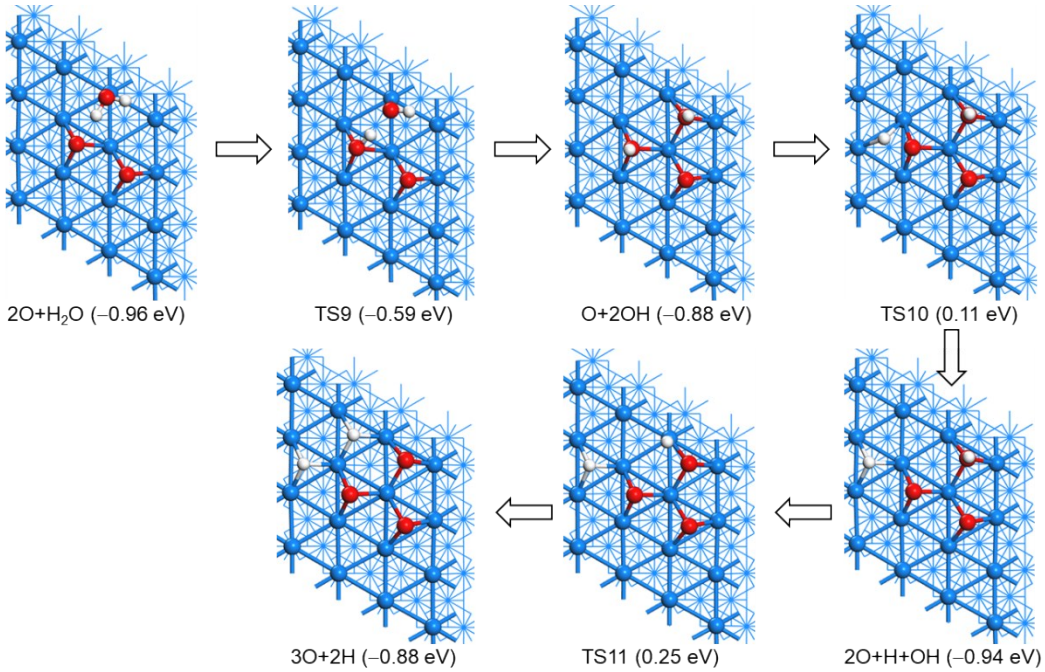

Figure S5. Optimized structures and the adsorption energy (eV) H_2O dissociation for the stationary points on the 3O pre-covered Ni(111) surface (Ni/blue; O/red; H/white)

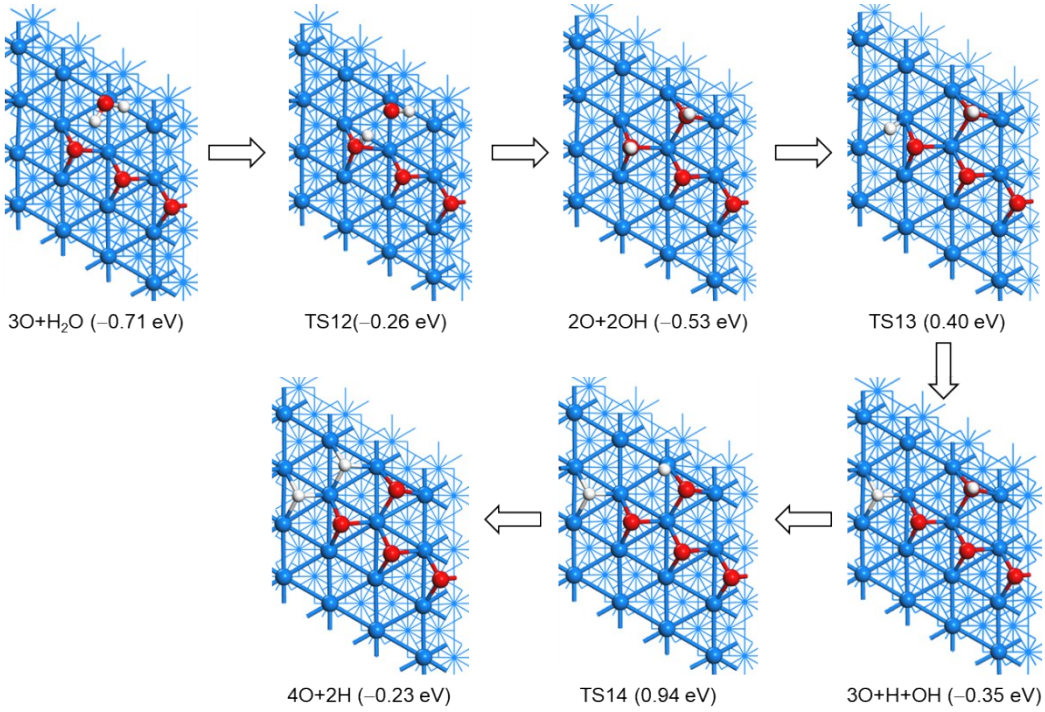

Figure S6. Optimized structures and the adsorption energy (eV) H_2O dissociation for the stationary points on the 4O pre-covered Ni(111) surface (Ni/blue; O/red; H/white)

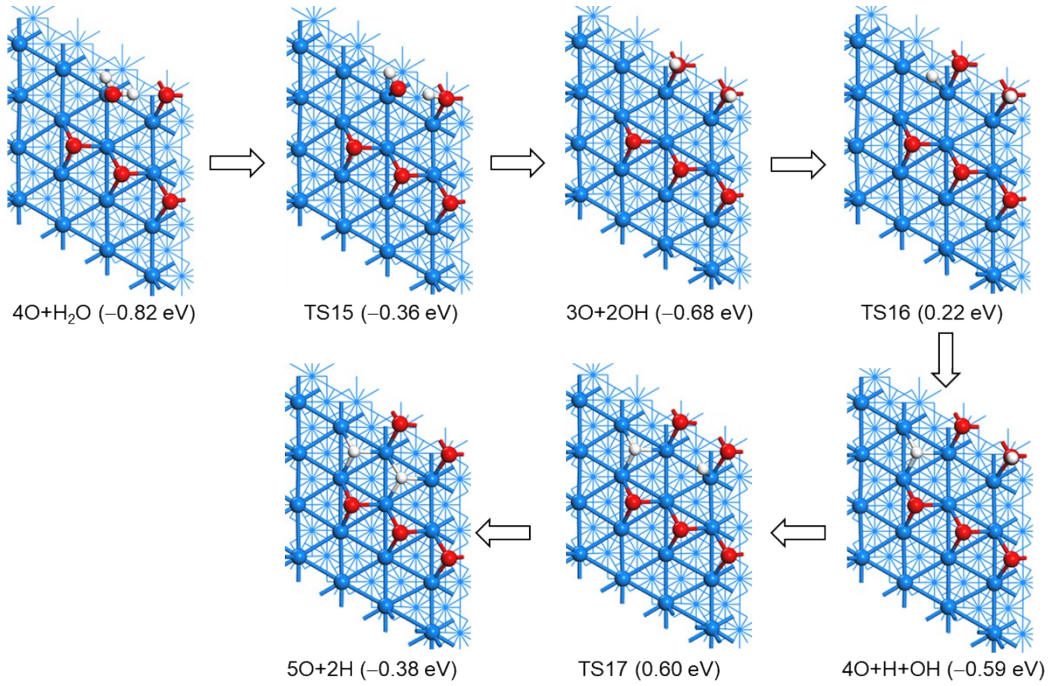

Figure S7. H_2O dissociation on nO (n = 3-4) pre-covered Ni(111) using PBE+D3 (the barrier of elementary steps in parentheses, the initial energy comes from the last step energy absorbed one more H_2O from gas phase, s for surface species, g for gas phase species)

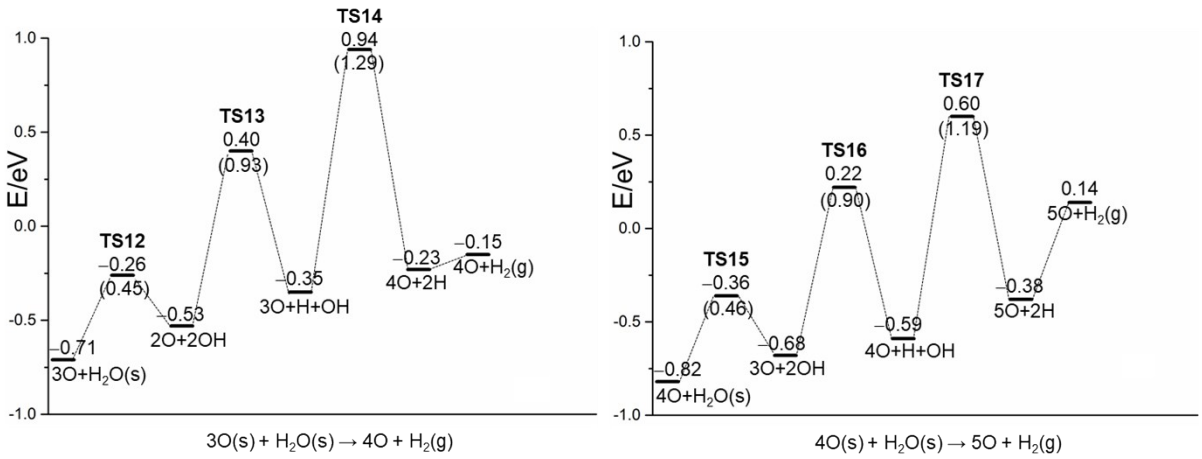

Figure S8. The computed 2OH configurations

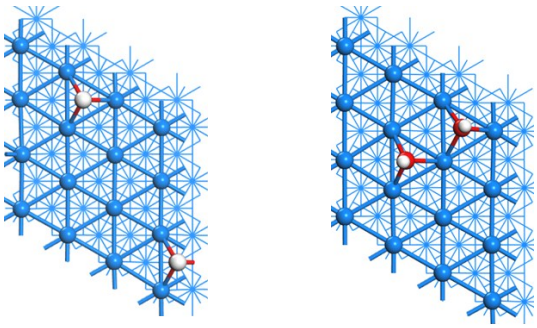

−6.47 eV −6.30 eV

Figure S9. The computed 4OH configurations

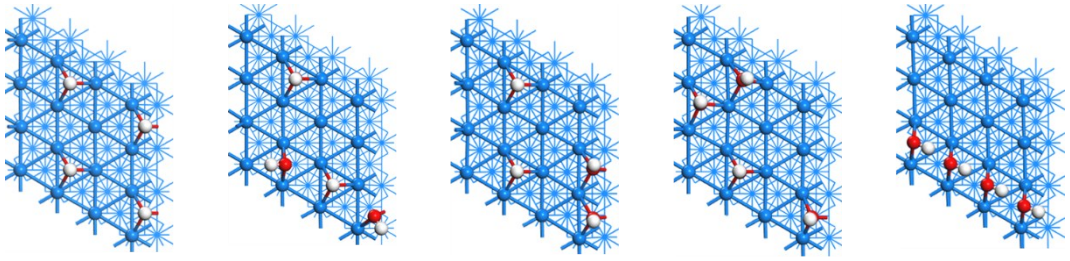

−12.76 eV −12.55 eV −12.55 eV −12.63 eV −12.35 eV

Figure S10. The computed 6OH configurations

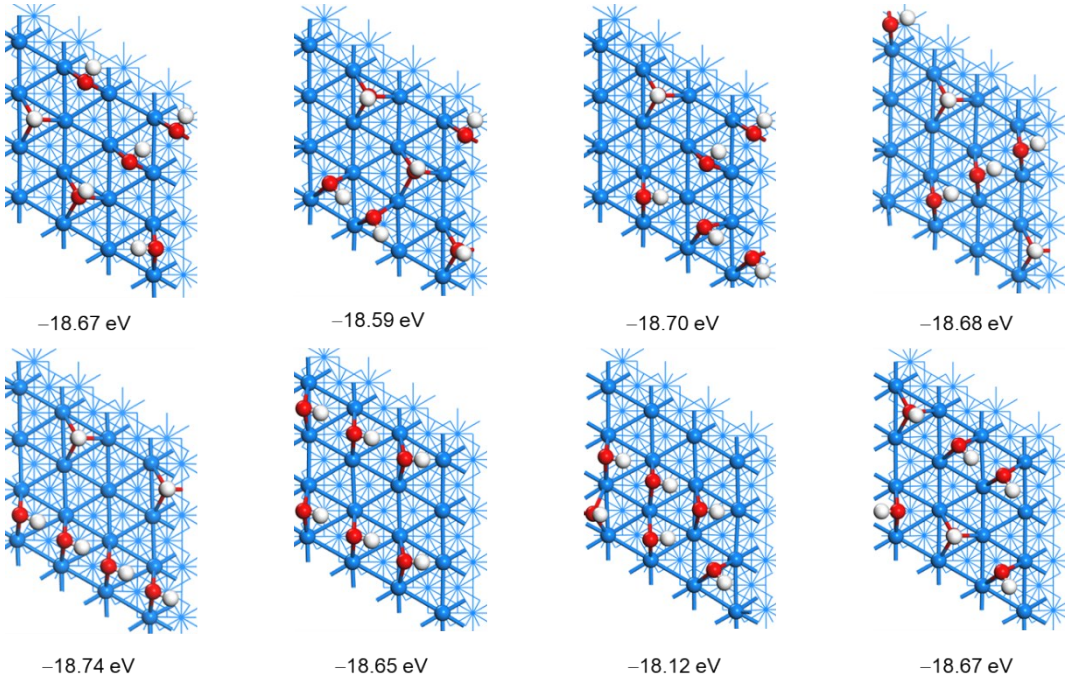

−18.67 eV −18.59 eV −18.70 eV −18.68 eV

−18.74 eV −18.65 eV −18.12 eV −18.67 eV

Figure S11. The computed 8OH configurations

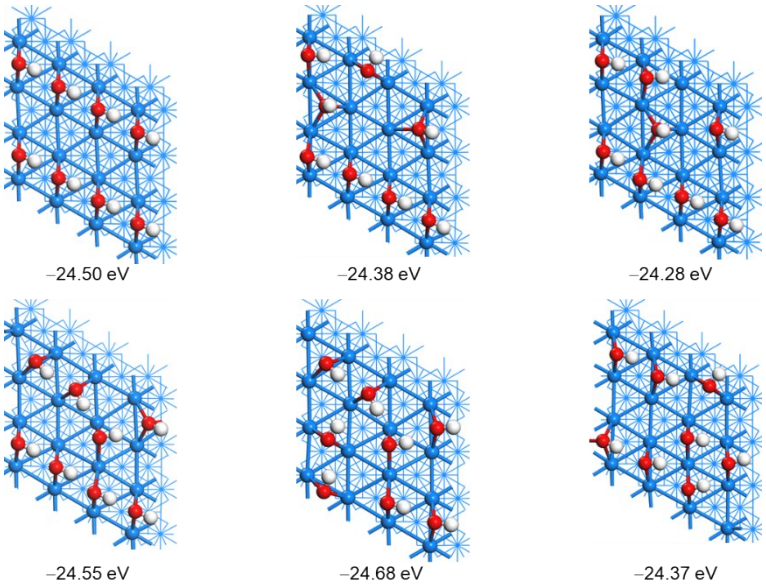

Figure S12. The computed 10OH, 12OH and 16 OH configurations

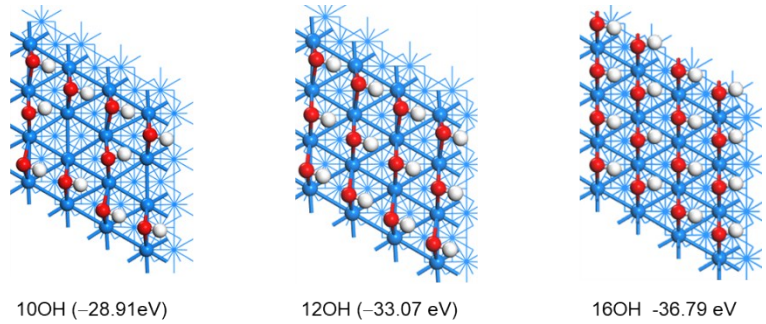

Figure S13. The computed 8O, 12O and 16O configurations